LighttTriggered cancer cell specific targeting and liposomal drug delivery in a zebrafish xenograft model

Kong, L.; Chen, Q.; Campbell, F.; Snaar-Jagalska, E.; Kros, A.

ADVANCED HEALTHCARE MATERIALS
www.advhealthmat.de

Light-Triggered Cancer Cell Specific Targeting and Liposomal Drug Delivery in a Zebrafish Xenograft Model

Li Kong, Quanchi Chen, Frederick Campbell, Ewa Snaar-Jagalska, and Alexander Kros**

Cell-specific drug delivery remains a major unmet challenge for cancer nanomedicines. Here, light-triggered, cell-specific delivery of liposome-encapsulated doxorubicin to xenograft human cancer cells in live zebrafish embryos is demonstrated. This method relies on light-triggered dePEGylation of liposome surfaces to reveal underlying targeting functionality. To demonstrate general applicability of this method, light-triggered, MDA-MB-231 breast cancer cell specific targeting in vivo (embryonic zebrafish) is shown using both clinically relevant, folate-liposomes, as well as an experimental liposome-cell fusion system. In the case of liposome-cell fusion, the delivery of liposomal doxorubicin direct to the cytosol of target cancer cells results in enhanced cytotoxicity, compared to doxorubicin delivery via either folate-liposomes or free doxorubicin, as well as a significant reduction in xenograft cancer cell burden within the embryonic fish.

1. Introduction

The majority (5 of 7) of clinically approved, targeted nanomedicines are liposomal formulations used to treat various human cancers.[1,2] All function through passive targeting of solid tumors via the enhanced permeability and retention (EPR) effect—a phenomenon characterized by the ill-defined ("leaky") vasculature and poor lymphatic drainage of select solid tumors.[3,4] To maximize passive targeting to solid tumors, PEGylation of nanoparticle surfaces is a long-standing strategy to reduce serum protein absorption, limit nanoparticle recognition and clearance by the reticulo-endothelial system (RES) in the liver and spleen, and prolong circulation lifetimes.[5,6] Once passively accumulated within the target tumor, however, drugs must be released from a nanoparticle at effective therapeutic concentrations (typically cytotoxic concentrations). In the case of Doxil (PEGylated liposomal doxorubicin)—the first clinically approved, targeted cancer nanomedicine—extracellular drug release relies on passive diffusion of doxorubicin across the liposome membrane. To maximize free drug concentrations within targeted tumors, methods to actively load very high concentrations of doxorubicin within liposomes have been developed.[7] Despite this, the superiority of clinically approved liposomal doxorubicin formulations, over administered free doxorubicin, remains contentious.[8] It is now generally accepted that improved toxicological profiles, rather than improved efficacy, constitute the main pharmacological benefit of liposomal-doxorubicin formulations (over administration of the free drug).

A potentially more effective strategy to treat cancer is to promote cellular uptake of drug-filled nanomedicines within cancer cells. This is most commonly attempted through the display of active targeting moieties (e.g., RGD, folate) from a nanoparticle surface.[9,10] However, active targeting strategies to promote cellular uptake of nanoparticles typically conflict with strategies employed to prolong circulation lifetimes. Most notably, the extremely limited cellular uptake of PEGylated nanoparticles hinders efficient intracellular drug delivery to cancer cells.[11] To overcome this PEG dilemma, stimuli-responsive dePEGylation of nanoparticles within the target tumor has been investigated.[12,13] In the majority of cases, dePEGylation is triggered by an endogenous stimuli (low pH,[14] matrix metalloproteinases[15]), exploiting pathophysiological differences between healthy and tumor tissues. However, suboptimal cleavage conditions/rates—common pH-sensitive groups (e.g., hydrazones, acetals, and benzoic imines) are optimally sensitive at pH <6, whereas the tumor microenvironment is generally pH >6.5[16]—typically lead to inefficient drug release profiles. Alternatively, dePEGylation of a nanoparticle can be triggered by an external stimuli, for example, light.[13] In this way, nanoparticle activation can be localized with very high spatiotemporal resolution, including deep within tissue. Two photon excitation sources, for example, can be used to focus light within femtoliter (fL) volumes at tissue depths of up to 1 cm,[17,18] while deeper tissues/pathologies can be accessed using fiber optic LEDs or injectable microLEDs.[19–21] Although the use of light to dePEGylate

Dr. L. Kong, Dr. F. Campbell, Prof. A. Kros
Supramolecular and Biomaterials Chemistry
Leiden Institute of Chemistry
Leiden University
Einsteinweg 55, 2333 CC Leiden, The Netherlands
E-mail: a.kros@chem.leidenuniv.nl

Q. Chen, Prof. E. Snaar-Jagalska
Institute of Biology
Leiden University
Leiden 2311 EZ, The Netherlands
E-mail: b.e.snaar-jagalska@biology.leidenuniv.nl

The ORCID identification number(s) for the author(s) of this article can be found under https://doi.org/10.1002/adhm.201901489.

DOI: 10.1002/adhm.201901489

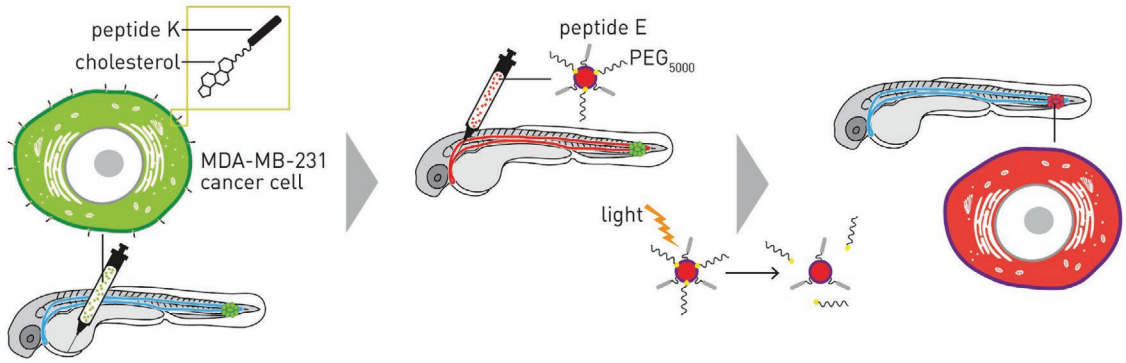

Figure 1. Light-triggered, cancer-cell-specific liposome–cell fusion in xenograft zebrafish embryos. Human cancer cells are first pre-functionalized with cholesterol–peptide K4 in vitro. Functionalized cancer cells are then injected into the circulation (via the duct of Cuvier) of 2-day old zebrafish embryos. Xenograft cancer cells quickly accumulate within the caudal hematopoietic tissue (CHT) of the embryo. One hour after cancer cell injection, EPEG-liposomes are injected into circulation via the posterior caudal vein (PCV). Prior to light-triggered dePEGylation, liposomes are confined to the vasculature of the fish and freely circulate. Following UV irradiation and in situ dePEGylation, liposomes rapidly and selectively bind to and fuse with xenograft cancer cells. This interaction is mediated through the recognition of fusogenic peptides E and K displayed from opposing lipid membranes. Liposome-encapsulated cargos (e.g., cytotoxic drugs) are delivered directly to the cytosol of the recipient cell.

nanomedicines has mainly been used to trigger extracellular drug release from a nanocarrier,[22–27] enhanced tumor targeting and active cellular uptake of dual responsive polymersomes following light activation has recently been reported.[28] In this case, near-infrared (NIR) light was used in combination with upconverting nanoparticles (UCNPs) to achieve efficient nanoparticle dePEGylation deep within a murine xenograft tumor.

Herein, we show light-triggered and cell-specific targeting of doxorubicin-filled liposomes to xenograft breast cancer cells in live embryonic zebrafish. Our method relies on responsive dePEGylation of a liposome surface, in situ and in vivo, to reveal underlying, active targeting functionality tethered to the liposome surface. To demonstrate the general applicability of this approach, we show light-triggered targeting of liposomal-doxorubicin formulations to cancer cells using both clinically relevant, folate-decorated liposomes (F-liposomes, targeting the overexpressed folate receptor on xenograft MDA-MB-231 cells[29,30]), as well as an experimental, two component (peptide E and K) fusion system that promotes direct fusion of liposome and cell membranes, with concurrent cytosolic delivery of encapsulated liposomal content (**Figure 1**).[31] For the fusion system, liposome–cell interactions rely on the recognition and binding of two coiled-coil forming peptides—peptide E (amino acid sequence: $(EIAALEK)_n$) and peptide K (*amino acid sequence*: $(KIAALKE)_n$)—tethered to opposing lipid membranes.[32] For this system to work, target cancer cell membranes must, therefore, first be enriched with the synthetic lipopeptide CPK (cholesterol-PEG_4-peptide K (see Scheme S1, Supporting Information, for chemical structure) to form K-functionalized cells. Once engrafted in vivo, these cells can recognize, bind to, and fuse with circulating liposomes whose membranes are enriched with the complementary lipopeptide, CPE (cholesterol-PEG_4-peptide E; see Scheme S1, Supporting Information, for chemical structure). Crucially, prior to light-triggered dePEGylation, both PEGylated E- and PEGylated F-liposomes freely circulated throughout the vasculature of the embryonic fish and did not interact either with xenograft cancer cells or key RES cell types of the embryo.

2. Results and Discussion

We have previously shown that the interaction between fusogenic peptides E and K, displayed from opposing membranes, can be sterically shielded through PEGylation of E-functionalized liposomes (E_{PEG}-liposomes).[33] Furthermore, through incorporation of a photocleavable linker, we have shown precise spatiotemporal control of liposome–liposome fusion and liposome–cell docking through light-triggered dePEGylation of E_{PEG}-liposomes in vitro.[34] In this case, PEG_{2000} was sufficient in length to sterically shield the interaction between complementary, three heptad (21 amino acid) E and K peptides (E_3 and K_3). However, to achieve full fusion of liposome and cell membranes, E and K peptides must be extended to four heptad repeats (E_4/K_4, 28 amino acids).[31]

To assess the optimal PEG length necessary to sterically shield the E_4/K_4 peptide interaction, lipid mixing experiments between E_4- and K_4-liposomes were, therefore, first performed in vitro (**Figure 2**a). For this, photolabile cholesterol-*o*-nitrobenzyl-PEG constructs (PEG_{2000} and PEG_{5000}; see Scheme S1, Supporting Information, for chemical structure) were incorporated (via post-modification), at varying mol% (0–10 mol%) within E_4-liposome formulations (see Supporting Information for size and zeta potentials of all liposomes, and Figure S1, Supporting Information, for TEM images of E_{PEG}- and F_{PEG}-liposomes). As photocleavable functionality, methoxy-functionalized *o*-nitrobenzyl groups were selected as: 1) they have been successfully used as photocage of a variety of bioactive compounds and biomolecules in complex biological solutions; 2) they have rapid photolysis kinetics; and 3), as the methyl substituted variant (at the benzylic position), the evolved nitroso photolytic by-products are less toxic than unsubstituted nitroso variants.[35] Now with larger tetrameric E_4 and K_4 peptides displayed from liposome surface, PEG_{2000} was shown ineffective at shielding the interaction between complementary peptides, as evidenced by significant lipid mixing of E- and K-liposome membranes even at high incorporated mol% of PEG. In contrast, >2 mol% cholesterol-PEG_{5000} incorporated within the

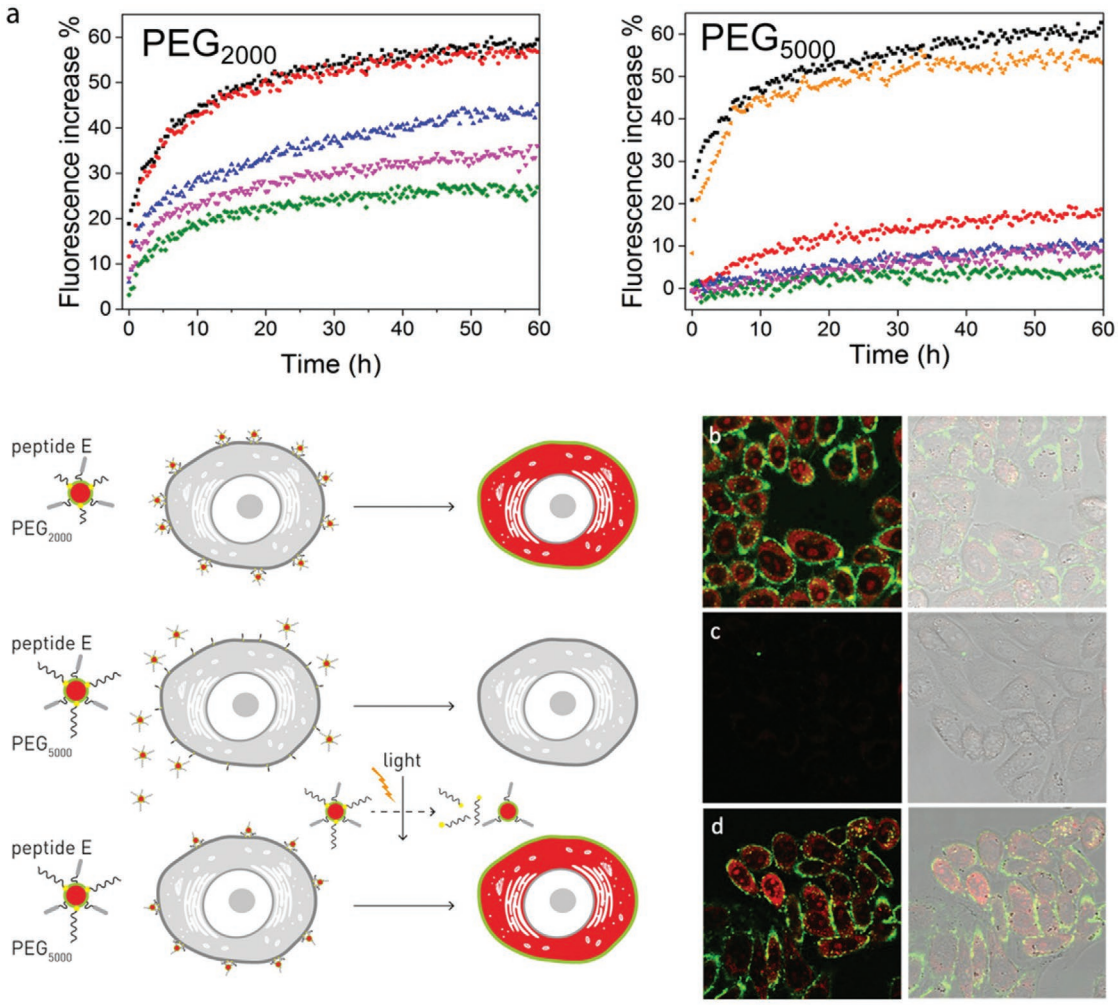

Figure 2. Optimization of required PEG length. a) Lipid mixing experiments of E- and K-liposomes incorporating varying mol% cholesterol-nitrobenzyl-PEG_{2000} (left) or cholesterol-nitrobenzyl-PEG_{5000} (right) within E-liposome formulations: 0 mol% (black), 2 mol% (red), 4 mol% (blue), 8 mol% (pink), 10 mol% (green) following UV irradiation (15 min, 370 ± 7 nm, 202 mW cm^{-2}) (orange). Liposome–cell fusion of E_{PEG}-liposomes: b) 4 mol% PEG_{2000} before UV; c,d) 4 mol% PEG_{5000} before and after applying UV light (15 min, 370 ± 7 nm, 50.6 mW cm^{-2}, light dose = 45.5 J cm^{-2}). E_{PEG}-liposomes contained 1 mol% DOPE-NBD (lipid probe, green) and encapsulated PI (75 μM, turn-on intercalator, red); scale bars = 30 μm.

E-liposome membrane was sufficient to completely shield the E4/K4 interaction. Furthermore, upon UV irradiation (15 min, 370 ± 7 nm, 202 mW cm^{-2}; see Figure S2, Supporting Information, for dePEGylation efficiency) of an equimolar solution of K-liposomes and E_{PEG}-liposomes (4 mol% photolabile cholesterol-PEG_{5000}), complete restoration of lipid mixing of K- and E-liposome membranes (Figure 2a) and a concomitant increase in liposome size, due to the fusion of two or more distinct liposomes (Figure S3, Supporting Information) was observed. Given the significantly smaller molecular size of folate, we assumed 4 mol% PEG_{5000} would be amply sufficient to sterically mask displayed folate functionality from the F-liposome surface. E_{PEG}-liposomes (containing 4 mol% photolabile cholesterol-PEG_{5000}) were stable in aqueous media (+10% serum) for at least 20 h at room temperature (Figure S4, Supporting Information).

Next, light-induced liposome–cell interactions, mediated through E/K complexation, were assessed in vitro (Figure 2b–d). For these experiments, HeLa cells were pre-functionalized with lipopeptide K_4 constructs (to form K-functionalized cells), as previously described.[36] E_{PEG}-liposomes (400 μM, 4 mol% PEG_{2000} or PEG_{5000})—containing a fluorescent lipid probe (1 mol% DOPE-NBD, green) and encapsulated propidium iodide (PI, a turn-on intercalator, 75 μM, red)—were incubated with K-functionalized cells, washed, and imaged, both before and after UV irradiation (15 min, 370 ± 7 nm, 50.6 mW cm^{-2}, light dose = 45.5 J cm^{-2}). Under analogous irradiation conditions and experimental setups, no photocytotoxicity was observed.[25] Supporting lipid mixing experiments, E_{PEG}-liposomes (PEG_{2000}, 4 mol%), prior to light irradiation, interacted with K-functionalized HeLa cells (Figure 2b), confirming PEG_{2000} is an insufficient steric shield in blocking E_4/K_4 interactions in both liposome–liposome and liposome–cell fusion experiments. In contrast, prior to light-triggered dePEGylation, E_{PEG}-liposomes (PEG_{5000}, 4 mol%) showed no interaction with cells nor intracellular PI delivery (Figure 2c). However, subsequent in situ UV irradiation (15 min, 370 ± 7 nm, 50.6 mW cm^{-2}, light dose = 45.5 J cm^{-2}) resulted in HeLa cell membranes homogenously labeled with

liposome-associated lipid probes (DOPE-NBD) and PI clearly dispersed within the cell cytosol (Figure 2d). Analogous localization and homogenous dispersion of lipid probes throughout target plasma cell membranes (rather than punctae within cells, indicative of endosomal uptake) was previously observed in E_4/K_4 mediated liposome–cell fusion experiments, including in the presence of various endocytosis inhibitors.[31] From these experiments, 4 mol% PEG_{5000} displayed on the surface of E_4-liposomes was deemed sufficient to inhibit putative E_4/K_4 mediated liposome–cell fusion and, by using photolabile lipid–PEG constructs, precise spatiotemporal control over liposome–cell membrane fusion could be achieved (Figure S5, Supporting Information).

Next, light-triggered, active targeting of liposomes to xenograft MDA-MB-231 breast cancer cells was assessed within live embryonic zebrafish (**Figure 3**). Both F-liposomes, targeting the overexpressed folate receptor on MDA-MB-231 cells,[29,30] and E-liposomes, targeting K-functionalized MDA-MB-231 cells, were independently tested. Zebrafish embryos are small (2–3 mm in length) and transparent enabling fluorescence imaging of specific biological events across entire living organisms in real time.[37] Zebrafish are increasingly used as model organisms to study fundamental processes such as embryogenesis, cell migration, sleep, and disease pathogenesis.[38–40] This includes the development of embryonic zebrafish xenograft models to study the pathogenesis of human cancers,[41–43] including human breast cancers.[44,45] Here, MDA-MB-231 breast cancer cells, stably expressing GFP, were microinjected into the circulation of 2-day old zebrafish larvae via the duct of Cuvier and quickly accumulated (<1 h post injection [hpi]) within the caudal hematopoietic tissue (CHT).[46] One hour after injection of cancer cells, either fluorescently labeled E_{PEG}- or F_{PEG}-liposomes (4 mol% PEG_{5000}, 1 mol% DOPE-LR probe) were injected (1 mM, 3 nL) into circulation via the posterior cardinal vein (PCV). Prior to UV irradiation, both E_{PEG}- and F_{PEG}-liposomes freely circulated, were confined within the vasculature of the embryo, and no co-localization of liposomes with either xenograft cancer cells or key RES cell types of the embryonic zebrafish (e.g., scavenging endothelial cells [SECs] or blood resident macrophages),[47] was observed (Figure 3).

Following in situ UV irradiation (15 min, 370 ± 7 nm, 13.5 mW cm^{-2}, light dose = 0.45 J per embryo) of the embryonic fish, however, both E- and F-liposomes rapidly and selectively co-localized with xenograft cancer cells (<30 min, i.e., prior to first image acquisition) (Figure 3). Under these irradiation conditions, embryos continued to develop normally (up to 6 days post-fertilization [dpf]) and no phenotypic abnormalities were observed (Figure S6, Supporting Information). Under identical conditions, the biodistribution of F_{PEG}-liposomes containing non-cleavable PEG_{5000} (DSPE-PEG_{5000}, Avanti) remained unchanged before and after in situ light irradiation, demonstrating the targeting requirement of both liposomes containing photocleavable PEG as well as UV light (Figure S7, Supporting Information). In the case of E-liposomes, E/K specificity was confirmed by repeating the experiment in the absence of peptide K (displayed from xenografted cancer cells). In this case, no E-liposome accumulation with cancer cells was observed following UV irradiation, confirming the requirement and selectivity of E_4/K_4 recognition and complexation for cell specific targeting (Figure S8, Supporting Information).

Extending our approach to liposome-mediated, intracellular drug delivery, we first measured the in vitro cytotoxicity (MDA-MB 231 cells, WST assay) of doxorubicin-filled E_{PEG}- and F_{PEG}-liposomes (4 mol% PEG_{5000}), before and after light activation, and compared this to the toxicity of free doxorubicin (**Figure 4**a). Again, for experiments involving E_{PEG}-liposomes, cells were first pretreated with lipopeptide K. For both E_{PEG}- and F_{PEG}-liposomes, cell viability was unaffected in the absence of applied UV light, and, in the case of E_{PEG}-liposomes, no intracellular DOX delivery was observed (Figure 4b; F_{PEG}-liposomes were not analyzed under the fluorescence microscope). Upon light-triggered dePEGylation, however, both E- and F-liposome mediated delivery of doxorubicin led to enhanced cytotoxicity (IC_{50} ≈100 and 200 μM, respectively, for E- and F-lipo-DOX) compared to free DOX (IC_{50} ≈300 μM). Interestingly, under these experimental conditions, the most potent cytotoxicity was observed for E/K-mediated liposomal delivery of DOX. This suggests DOX delivery direct to the cell cytosol, following liposome-cell membrane fusion, is a potentially potent method of drug delivery. Importantly, freshly prepared DOX-loaded liposomes used in all cases, as significant DOX leakage (30-40%) from the liposome core was observed for all formulations during prolonged storage and would affect the efficiency of liposomal DOX delivery over time (Figure S9, Supporting Information).

Next, doxorubicin-filled E_{PEG}-liposomes (4 mol% PEG_{5000}, 250 μM doxorubicin) were intravenously microinjected into embryonic zebrafish xenografts (K-functionalized MDA-MB-231 breast cancer cells) (Figure 4c) and the efficacy in reducing tumor burdens assessed (Figure 4d,e). For this, relative cancer cell proliferation was quantified by measuring total GFP fluorescence of xenograft cancer cells. Here, significantly ($p < 0.0001$) reduced cancer cell proliferation (46.9% reduction) was only observed in the "+UV" group. In the absence of light, tumor proliferation was unaffected and no significant difference in cancer cell numbers was measured compared to the untreated controls. Again, using cancer cells unfunctionalized with peptide K, no reduction in cancer cell proliferation was observed (Figure S10, Supporting Information), further emphasizing the essential requirement and selectivity of E_4/K_4 recognition and complexation.

3. Conclusion

Here, we successfully demonstrate light-triggered targeting of liposomes to xenograft cancer cells in vivo. Our approach relies on the light-triggered dePEGylation of liposome surfaces, revealing underlying targeting functionality. General applicability of this approach was demonstrated using both an experimental two-component fusion system (peptides E and K) as well as clinically relevant folate-decorated liposomes. Both E_{PEG}- and F_{PEG}-liposomes, prior to light-triggered activation, freely circulated throughout the vasculature of the embryonic zebrafish, and showed no significant interactions with either target cancer cells or key RES cell types (scavenging endothelial cells or blood resident macrophages) within the fish.[47] In mammals, analogous RES cell types, namely liver sinusoidal endothelial cells (LSECs), Kupffer cells (hepatic, blood resident macrophages), and splenic macrophages, are responsible for the clearance of the majority of i.v. administered nanoparticles

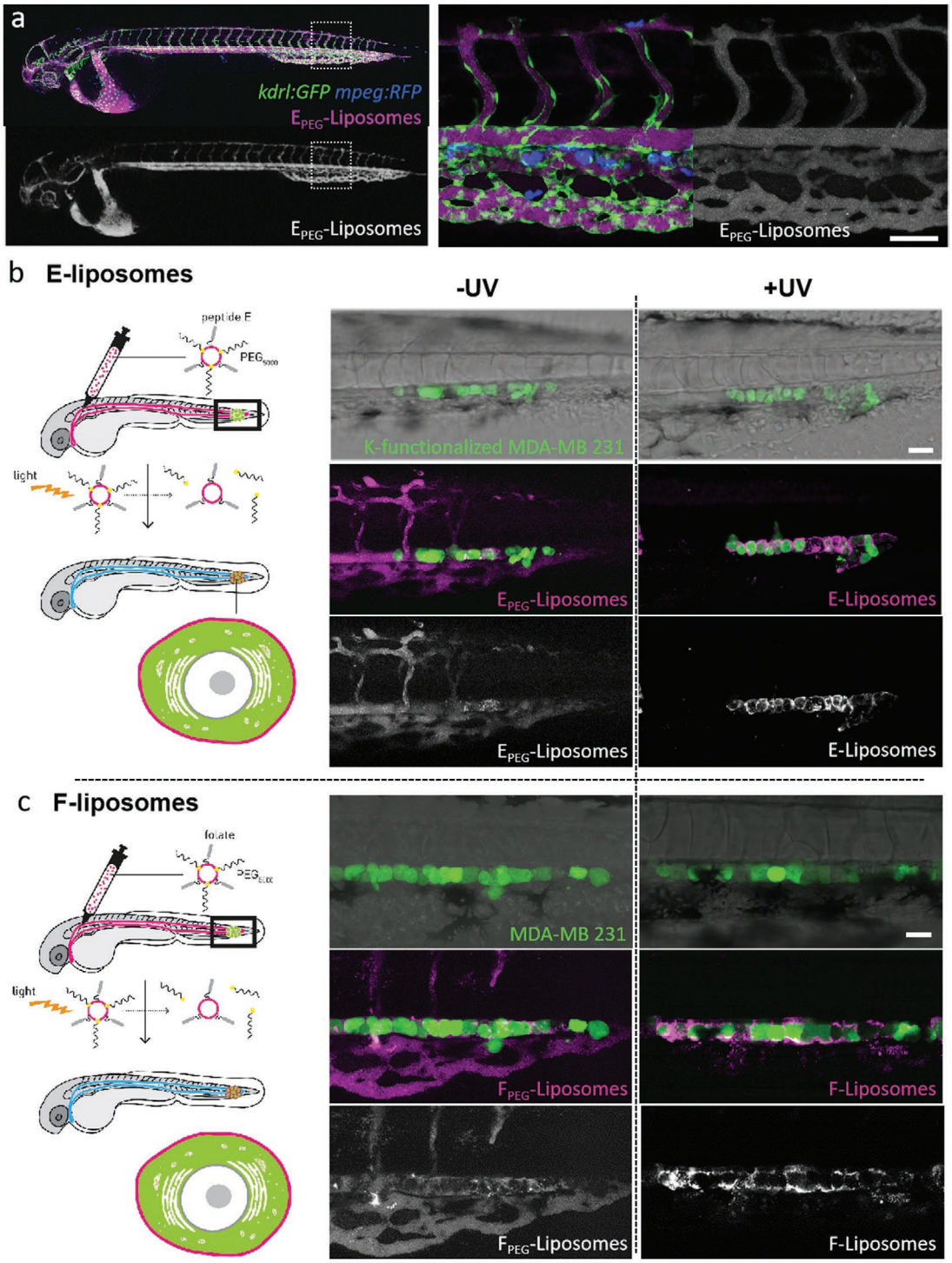

Figure 3. Cancer cell specific, light-triggered liposome–cell interactions in vivo. a) Biodistribution of E_{PEG}-liposomes (1 mM, 4 mol% PEG_{5000}, containing 1 mol% DOPE-Atto 633, far red) in *Tg(kdrl:GFP/mpeg:RFP)* zebrafish embryos (2 dpf), following i.v. injection. Liposomes are confined within the vasculature of the embryo and freely circulate. No liposome co-localization with either endothelial cells (green) or (blood resident) macrophages (blue) is observed indicative of the ability of E_{PEG}-liposomes to evade key RES cell types. Confocal z-stacks acquired at 1hpi. b,c) MDA-MB-231 human breast cancer cells, stably expressing GFP, were injected into the circulation of a 2-day old zebrafish embryo and quickly accumulated in the caudal hematopoietic tissue (CHT). In the case of E-liposomes, cells were pre-treated with lipopeptide K. Into this xenograft model, either E_{PEG}- or F_{PEG}-liposomes (1 mM, 4 mol% PEG_{5000}, containing 1 mol% DOPE-LR, red) were injected into circulation. Prior to UV irradiation, both E_{PEG}- or F_{PEG}-liposomes were freely circulating, confined within the vasculature of the fish (left image panels). Following UV irradiation (15 min, 370 ± 7 nm, 13.5 mW cm^{-2}, light dose = 0.45 J per embryo) and photolytic dePEGylation, both E- and F-liposomes selectively bound to xenograft cancer cells within the CHT (right image panels). Data are representative of three independent experiments (each $n = 5$). Field of view = boxed region in embryo cartoon. Scale bars = 100 µm.

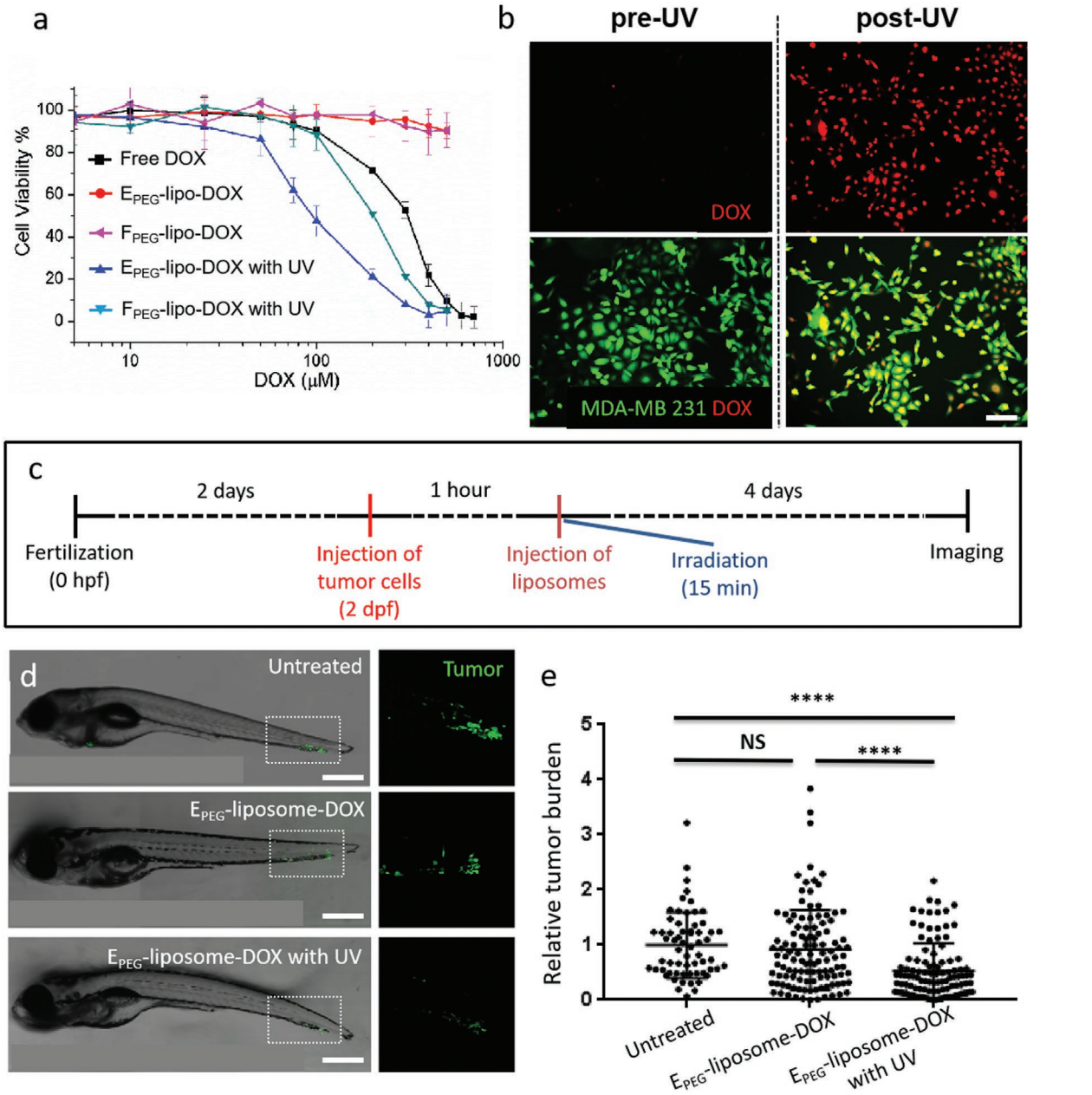

Figure 4. Delivery of liposome-encapsulated doxorubicin to MDA-MB 231 cells both in vitro and in vivo. a) MDA-MB-231 breast cancer cell viability in vitro (measured by WST assay) following 2 h incubation with either DOX-filled E_{PEG}-liposomes (4 mol% PEG_{5000}), before (red) and after (blue) UV activation (15 min, 370 ± 7 nm, 50.6 mW cm^{-2}, light dose = 45.5 J cm^{-2}); F_{PEG}-liposomes (4 mol% PEG_{5000}), before (pink) and after (cyan) UV activation; or free doxorubicin (black) without UV irradiation. For +UV samples, liposomes were added to cells and immediately irradiated. 2 h incubation time includes 15 min irradiation time. In the absence of light, both E_{PEG}- and F_{PEG}-lipo-DOX formulations were non-toxic. Following light activation, liposome-mediated delivery of doxorubicin resulted in enhanced cytotoxicity (F-liposomes, IC_{50} = approx. 200 μM; E-liposomes, IC_{50} = approx. 100 μM) compared to free doxorubicin (IC_{50} = approx. 300 μM). In all cases, freshly prepared DOX-filled liposomes were used to minimize the effects of DOX leakage over time. b) Intracellular DOX delivery by E_{PEG}-liposomes (200 μM encapsulated DOX, red) and K-functionalized MDA-MB-231 breast cancer cells, stably expressing GFP, green, before (left) and after (right) UV irradiation (15 min, 370 ± 7 nm, 50.6 mW cm^{-2}, light dose = 45.5 J cm^{-2}). Scale bars = 100 μm. c) Timeline of zebrafish development, MDA-MB-231 cell injection, liposome injection, and quantification in the zebrafish embryo. At 2 dpf, MDA-MB-231 cells (approx. 300 cells) were injected into circulation via the duct of Cuvier. One hour after engraftment, DOX-filled, E_{PEG}-liposomes (3 nL, 4 mM total lipid; 200 μM encapsulated doxorubicin) were injected into circulation via the posterior cardinal vein. UV irradiation (15 min, 370 ± 7 nm, 13.5 mW cm^{-2}, light dose = 0.45 J per embryo), where appropriate, was performed immediately after the injection of liposomes. Tumor burden analyzed at 4 dpi. d,e) Visualization and quantification of cancer proliferation in the zebrafish embryo. Significant ($p < 0.0001$) reduction in tumor volume was only observed for DOX-filled, E_{PEG}-liposomes, following in situ light activation. In the absence of light activation, tumor progression/burden was unaffected as for untreated controls. Data is presented as mean values ± SD; each point on the scatter plots represents one larva. Brackets indicate significantly different values (****, $p < 0.0001$; NS, not significant) based on one-way ANOVA statistical testing. $n = 61$ individually injected embryos (untreated group). $n = 114$ (without UV group) and $n = 108$ (with UV group). Scale bars = 500 μm.

from the body.[48] While there is currently no established model for the EPR effect in embryonic zebrafish, the implications of our findings are that both E_{PEG}- and clinically relevant F_{PEG}-liposomes, prior to light activation, would likely evade RES clearance in mammals, prolonging circulation lifetimes and the potential for liposome accumulation in pathological tissues with enhanced permeability.

In the case of E-liposome targeting, prior modification of cancer cell membranes with complementary peptide K is a pre-requisite. While this system provides us with a fundamental tool to probe alternative liposomal drug delivery routes (i.e., fusion versus endocytosis), as well as a highly selective handle for targeting as is shown in this study, the necessity for components displayed from both liposome and target cell membranes is a major limitation to further in vivo application. Similarly, the use of UV light as a trigger raises valid concerns over applicability in larger, non-transparent mammals, including humans. To some extent, these concerns relate to the poor tissue penetration of UV light (≈100–200 µm). As a result, the clinical use of UV light is restricted to the topical treatment of cosmetic skin disorders, including psoriasis, acne, and eczema.[49] However, these limitations are increasingly being overcome, as fundamental advances in fiber optic[19] and wireless LED technologies[20,21] facilitate the localized delivery of UV light deep within patients. Alternatively, extended exposure to UV light is known to pose a significant health risk, with the potential to cause DNA damage, cytotoxicity, and cancer.[50] In this study, applied UV-A (370 ± 7 nm) light doses to zebrafish embryos (12.1 J cm^{-2}) are well below recommended (skin) exposure limits (32 J cm^{-2} @ 375 nm).[51] Furthermore, while single photon UV-A (370 nm) light is optimal for the photolysis of *o*-nitrobenzyl functionalities, the use of 2-photon excitation sources[52,53] or photolabile chemistries sensitive to longer wavelength, visible light,[54,55] offer options for light activation both deep in tissue and with reduced photocytotoxicity.

Finally, this study highlights the unique opportunities offered by the embryonic zebrafish model in the design and optimization of nanomedicines. In this study, we were able to generate our desired xenograft cancer model without the need for immunosuppression (the adaptive immune system is not yet developed zebrafish embryos); directly visualize the changing pharmacokinetics of stimuli-responsive nanoparticles in situ, in vivo, and in real time; and set-up and perform efficacy studies, involving several hundred animals, within 1 week. The combined level of detailed assessment, low cost, and experimental speed, afforded by the embryonic zebrafish model, is simply not achievable using conventional animal models (e.g., mice and rats). As to the predictive potential of the embryonic zebrafish, we, and others, have recently shown both pharmacokinetic parameters and key cellular interactions of nanomedicines are highly conserved between the embryonic zebrafish and mice.[47,56]

Supporting Information

Supporting Information is available from the Wiley Online Library or from the author.

Acknowledgements

L.K. and Q.C. contributed equally to this work. This work was funded through the Chinese Scholarship Council grants (L.K. and Q.C.) and the Netherlands Organization for Scientific Research (NWO-Vici-project nr. 724.014.001; F.C. and A.K.). Arwin Groenewoud (Institute of Biology, Leiden University) is thanked for the kind gift of Plasmid #106172 (Addgene.org). Infographics were developed by Joost Bakker (www.scicomvisuals.com). Zebrafish (*Danio rerio*, strain AB/TL) were maintained and handled according to the guidelines from the Zebrafish Model Organism Database (http://zfin.org) and in compliance with the directives of the local animal welfare committee of Leiden University.

Conflict of Interest

The authors declare no conflict of interest.

Keywords

cancer nanomedicine, embryonic zebrafish, in vivo, light activation, liposomes

Received: October 21, 2019
Revised: January 2, 2020
Published online: February 13, 2020

[1] C. L. Ventola, *P T* **2017**, *42*, 742.
[2] J. Shi, P. W. Kantoff, R. Wooster, O. C. Farokhzad, *Nat. Rev. Cancer* **2017**, *17*, 20.
[3] H. Maeda, J. Wu, T. Sawa, Y. Matsumura, K. Hori, *J. Controlled Release* **2000**, *65*, 271.
[4] H. Maeda, H. Nakamura, J. Fang, *Adv. Drug Delivery Rev.* **2013**, *65*, 71.
[5] M. L. Immordino, F. Dosio, L. Cattel, *Nanomedicine* **2006**, *1*, 297.
[6] J. S. Suk, Q. Xu, N. Kim, J. Hanes, L. M. Ensign, *Adv. Drug Delivery Rev.* **2016**, *99*, 28.
[7] A. Fritze, F. Hens, A. Kimpfler, R. Schubert, R. Peschka-Süss, *Biochim. Biophys. Acta, Biomembr.* **2006**, *1758*, 1633.
[8] Y. Ngan, M. Gupta, *Arch. Pharm. Pract.* **2016**, *7*, 1.
[9] J. D. Byrne, T. Betancourt, L. Brannon-Peppas, *Adv. Drug Delivery Rev.* **2008**, *60*, 1615.
[10] R. Bazak, M. Houri, S. El Achy, S. Kamel, T. Refaat, *J. Cancer Res. Clin. Oncol.* **2015**, *141*, 769.
[11] S. Mishra, P. Webster, M. E. Davis, *Eur. J. Cell Biol.* **2004**, *83*, 97.
[12] Y. Fang, J. Xue, S. Gao, A. Lu, D. Yang, H. Jiang, Y. He, K. Shi, *Drug Delivery* **2017**, *24*, 22.
[13] L. Kong, F. Campbell, A. Kros, *Nanoscale Horiz.* **2019**, *4*, 378.
[14] B. A. Webb, M. Chimenti, M. P. Jacobson, D. L. Barber, *Nat. Rev. Cancer* **2011**, *11*, 671.
[15] C. Mehner, A. Hockla, E. Miller, S. Ran, D. C. Radisky, E. S. Radisky, *Oncotarget* **2014**, *5*, 2736.
[16] P. Vaupel, F. Kallinowski, P. Okunieff, *Cancer Res.* **1989**, 6449.
[17] A. Karotki, M. Khurana, J. R. Lepock, B. C. Wilson, *Photochem. Photobiol.* **2006**, *82*, 443.
[18] F. Bolze, S. Jenni, A. Sour, V. Heitz, *Chem. Commun.* **2017**, *53*, 12857.
[19] S. H. Yun, S. J. J. Kwok, *Nat. Biomed. Eng.* **2017**, *1*, 8.
[20] T. Il Kim, J. G. McCall, Y. H. Jung, X. Huang, E. R. Siuda, Y. Li, J. Song, Y. M. Song, H. A. Pao, R. H. Kim, C. Lu, S. D. Lee, I.-S. Song, G. C. Shin, R. Al-Hasani, S. Kim, M. P. Tan, Y. Huang, F. G. Omenetto, J. A. Rogers, M. R. Bruchas, *Science* **2013**, *340*, 211.
[21] A. Bansal, F. Yang, T. Xi, Y. Zhang, J. S. Ho, *Proc. Natl. Acad. Sci. USA* **2018**, *115*, 1469.

[22] J. Wang, Y. Ouyang, S. Li, X. Wang, Y. He, *RSC Adv.* **2016**, *6*, 57227.
[23] G. Saravanakumar, H. Park, J. Kim, D. Park, S. Pramanick, D. H. Kim, W. J. Kim, *Biomacromolecules* **2018**, *19*, 2202.
[24] Q. Jin, T. Cai, H. Han, H. Wang, Y. Wang, J. Ji, *Macromol. Rapid Commun.* **2014**, *35*, 1372.
[25] L. Kong, D. Poulcharidis, G. F. Schneider, F. Campbell, A. Kros, *Int. J. Mol. Sci.* **2017**, *18*, 2033.
[26] D. Zhou, J. Guo, G. B. Kim, J. Li, X. Chen, J. Yang, Y. Huang, *Adv. Healthcare Mater.* **2016**, *5*, 2493.
[27] N. Kalva, N. Parekh, A. V. Ambade, *Polym. Chem.* **2015**, *6*, 6826.
[28] M. Zhou, H. Huang, D. Wang, H. Lu, J. Chen, Z. Chai, S. Q. Yao, Y. Hu, *Nano Lett.* **2019**, *19*, 3671.
[29] L. C. Hartmann, G. L. Keeney, W. L. Lingle, T. J. H. Christianson, B. Varghese, D. Hillman, A. L. Oberg, P. S. Low, *Int. J. Cancer* **2007**, *121*, 938.
[30] R. Meier, T. D. Henning, S. Boddington, S. Tavri, S. Arora, G. Piontek, M. Rudelius, C. Corot, H. E. Daldrup-Link, *Radiology* **2010**, *255*, 527.
[31] J. Yang, A. Bahreman, G. Daudey, J. Bussmann, R. C. L. Olsthoorn, A. Kros, *ACS Cent. Sci.* **2016**, *2*, 621.
[32] H. Robson Marsden, N. A. Elbers, P. H. H. Bomans, N. A. J. M. Sommerdijk, A. Kros, *Angew. Chem., Int. Ed.* **2009**, *48*, 2330.
[33] I. Tomatsu, H. R. Marsden, M. Rabe, F. Versluis, T. Zheng, H. Zope, A. Kros, *J. Mater. Chem.* **2011**, *21*, 18927.
[34] L. Kong, S. H. C. Askes, S. Bonnet, A. Kros, F. Campbell, *Angew. Chem., Int. Ed.* **2016**, *55*, 1396.
[35] P. Klán, T. Šolomek, C. G. Bochet, A. Blanc, R. Givens, M. Rubina, V. Popik, A. Kostikov, J. Wirz, *Chem. Rev.* **2013**, *113*, 119.
[36] H. R. Zope, F. Versluis, A. Ordas, J. Voskuhl, H. P. Spaink, A. Kros, *Angew. Chem., Int. Ed.* **2013**, *52*, 14247.
[37] S. Sieber, P. Grossen, J. Bussmann, F. Campbell, A. Kros, D. Witzigmann, J. Huwyler, *Adv. Drug Delivery Rev.* **2019**, *151–152*, 152.
[38] C. Santoriello, L. I. Zon, *J. Clin. Invest.* **2012**, *122*, 2337.
[39] R. Jones, *PLoS Biol.* **2007**, *5*, 2103.
[40] M. R. Cronan, D. M. Tobin, *Dis. Models Mech.* **2014**, *7*, 777.
[41] C. Grabher, A. T. Look, *Nat. Biotechnol.* **2006**, *24*, 45.
[42] M. Konantz, T. B. Balci, U. F. Hartwig, G. Dellaire, M. C. André, J. N. Berman, C. Lengerke, *Ann. N. Y. Acad. Sci.* **2012**, *1266*, 124.
[43] Y. Drabsch, B. E. Snaar-Jagalska, P. Ten Dijke, *Histol. Histopathol.* **2017**, *32*, 673.
[44] C. Tulotta, C. Stefanescu, E. Beletkaia, J. Bussmann, K. Tarbashevich, T. Schmidt, B. E. Snaar-Jagalska, *Dis. Models Mech.* **2016**, *9*, 141.
[45] Y. Drabsch, S. He, L. Zhang, B. E. Snaar-Jagalska, P. ten Dijke, *Breast Cancer Res.* **2013**, *15*, R106.
[46] M. De Boeck, C. Cui, A. A. Mulder, C. R. Jost, S. Ikeno, P. Ten Dijke, *Sci. Rep.* **2016**, *6*, 24968.
[47] F. Campbell, F. L. Bos, S. Sieber, G. Arias-Alpizar, B. E. Koch, J. Huwyler, A. Kros, J. Bussmann, *ACS Nano* **2018**, *12*, 2138.
[48] Y. N. Zhang, W. Poon, A. J. Tavares, I. D. McGilvray, W. C. Chan, *J. Controlled Release* **2016**, *240*, 332.
[49] R. Vangipuram, S. R. Feldman, *Oral Diseases* **2016**, *22*, 253.
[50] D. L. Narayanan, R. N. Saladi, J. L. Fox, *Int. J. Dermatol.* **2010**, *49*, 978.
[51] R. Matthes, *Health Phys.* **2004**, 171.
[52] T. Furuta, S. S.-H. Wang, J. L. Dantzker, T. M. Dore, W. J. Bybee, E. M. Callaway, W. Denk, R. Y. Tsien, *Proc. Natl. Acad. Sci. U. S. A.* **1999**, *96*, 1193.
[53] K. Peng, I. Tomatsu, A. V. Korobko, A. Kros, *Soft Matter* **2010**, *6*, 85.
[54] V. Shanmugam, S. Selvakumar, C.-S. Yeh, *Chem. Soc. Rev.* **2014**, *43*, 6254.
[55] I. Aujard, C. Benbrahim, M. Gouget, O. Ruel, J. B. Baudin, P. Neveu, L. Jullien, *Chem. - Eur. J.* **2006**, *12*, 6865.
[56] S. Sieber, P. Grossen, P. Detampel, S. Siegfried, D. Witzigmann, J. Huwyler, *J. Controlled Release* **2017**, *264*, 180.